Targeted nanotheranostics for personalized cancer therapy

Odile Diou, Nicolas Tsapis & Elias Fattal†

†*University Paris-Sud, Institut Galien Paris-Sud, UMR CNRS 8612, LabEx LERMIT, Facult de Pharmacie, 5 rue Jean-Baptiste Clément, Châtenay-Malabry, France*

Introduction: The development of nanomedicine, during the last 10 years have given rise to novel delivery systems among which multifunctional platforms called nanotheranostics that are designed to simultaneously diagnose and cure cancer. These systems can be built using the large panel of biocompatible and biodegradable materials. The recent advances of imaging modalities even enable targeted nanotheranostics to probe molecular structures on specific cells opening the doors to personalized cancer therapy.

Areas covered: This review presents the different requirements nanotheranostics should fulfill to achieve an optimized anticancer therapy. It focuses on two imaging modalities: MRI and ultrasonography used to visualize drug delivery, release, and efficacy. The advantages and limitations of these two methods are considered. The review will enable the readers to virtually tune a nanotheranostic system according to the nature of the targeting tissue and the availability of imaging modality.

Expert opinion: Despite great perspectives, described for nanotheranostic systems in personalized cancer therapy, the imaging techniques still face technological issues, such as high sensitivity and good spatial and temporal resolutions. Active targeting should consider better specificity and low immunogenicity of the ligand selected, to be more efficient.

Keywords: 19F MRI, 1H MRI, chemotherapy, drug efficacy monitoring, nanotheranostics, personalized medicine, stimuli-sensitive release, ultrasonography

Expert Opin. Drug Deliv. (2012) 9(12):1475-1487

1. Introduction

Cancer results from uncontrolled growth of mutated cells in the body. The disease is characterized by i) a rapid proliferation of genetically altered cells, which access to immortality, ii) the invasion of adjacent tissues by creating a network of anarchical blood vessels (angiogenesis), and in some cases iii) the spreading of malignancy in other parts of the body (metastasis). According to the most recent numbers, provided by the GLOBOCAN project, 7.6 million people have died from cancer (13% of all death) in 2008. Pessimistic predictions, from the International Agency for Research on Cancer, raise the number of cancer incidence from 12.7, in 2008, to 21.3 million in 2030. By now, the methods, used for detection and treatment, lack effectiveness and specificity, and most of the anticancer drugs induce side effects. Furthermore, when the treatment fails, the absence of satisfying modality for treatment monitoring and feedback slows down the decision making to change the strategy.

Nanotheranostic systems were recently developed to overcome these problems. The word theranostic was first mentioned in the literature in 2002 and has been the topic of around 270 papers during this last decade. Nanotheranostic platforms are designed to image nanocarrier's biodistribution, to survey and map the extent of disease, to deliver the treatment, and to monitor in real time the mechanism of

10.1517/17425247.2012.736486 © 2012 Informa UK, Ltd. ISSN 1742-5247

Article highlights.

- The use of nanotheranostic systems involves earlier and improved detection of cancer and designed treatment protocol, to envision personalized cancer therapy.
- In the literature, the nanotheranostic systems are numerous. They basically consist of a carrier, an imaging label, and a bioactive molecule. Different examples of each component are given in the review.
- Two tumor-targeting strategies are possible and can be combined for better efficacy of nanotheranostic systems: active and passive targeting.
- Ultrasonography and MRI are noninvasive imaging modalities and can be used separately or in association with each other (MR-HIFU). In combination with nanotheranostic systems, the techniques allow to image the tumor and activate or monitor the drug release.
- The perfluorocarbons (PFCs) form one particular interesting imaging probe family. PFCs can be used for ultrasonography as well as for MRI. PFCs are taken up by cells to track them *in vivo* and design systems for cancer immunotherapy. The unique physicochemical properties of PFCs enable performing oxymetry measurements and enriching the acoustic response.
- The limitations of MRI are the spatial resolution and the potential time-consuming acquisition (^{19}F MRI). The limitations of ultrasonography are the low sensitivity and the inability to image organs such as lungs and brain.

This box summarizes key points contained in the article.

action and the efficacy of treatment [1,2]. In brief, treatment will be tailored to "Administer the right drug to the right patient at the right moment" [3].

Nanotheranostic systems typically consist of a carrier, an imaging label and a bioactive molecule, such as a target-specific entity or chemotherapeutic drug (**Figure 1**). The carrier at best should be made of biodegradable and biocompatible materials, because the mechanisms of degradation and elimination are more predictable, and toxicity is better controlled. This is the case of liposomes and the majority of polymeric nanoparticles, whereas other types of materials, with unknown biological issues, have been used to design dendrimers, carbon nanotubes, or Metal Organic Frameworks. The carrier also provides an optimal biodistribution and delivers two payloads: the imaging probe (metallic nanoparticles, quantum dots, fluorophores, etc.) and the bioactive molecule (peptides, proteins, nucleic acids, or chemotherapeutic drugs). Many reviews already referenced the numerous possible combinations of these three elements, their synthesis, and features [4-6].

This review will focus on nanotheranostics in combination with two complementary and noninvasive imaging modalities: Ultrasonography and Magnetic Resonance Imaging (MRI). Ultrasonography is cost-effective, portable, and provides real-time anatomical information. MRI imparts deep penetration into soft tissues with high contrast and better sensitivity. Both these techniques have been used to directly treat, activate, or monitor the therapy. A special attention will be given here to ^{19}F MRI, which is a recently developed but very promising technique. It offers excellent signal-to-noise ratio and eases the quantification of contrast agent or therapeutic molecules [7]. ^{19}F MRI is not commonly used in clinics because radiofrequency coils, tuned for fluorine are not commercialized yet, their construction building process is still at the academic stage [8]. ^{19}F MRI can be combined with ^{1}H MRI to obtain anatomical information [9].

We will first present the physiological barriers encountered by the nanotheranostics after systemic administration and how they can be overcome. We will then discuss the different strategies, which are currently developed for tumor targeting and show how nanotheranostics can report the tumor condition. Finally, we will provide an overview of the therapeutic approaches to treat malignant tissues. In brief, the different abilities of nanotheranostic systems will be described at each step, from injection to evaluation of treatment efficacy.

2. Nanotheranostics overcome the physiological barriers

After intravenous injection, nanotheranostic systems are subjected to several physiological processes and mass transfers within the body. They may be removed or destroyed before reaching the targeted disease site. It is therefore very important to understand the role of physiological barriers to predict the fate of exogenous nanotheranostics and their biodistribution.

Nanotheranostics are usually prepared as suspension in water or buffer solution. *In vitro* stability measurements, assessed in different media, allow predicting stability issues that could arise after administration [10]. Aggregation, hydrolysis, or cleavage of the nanotheranostic may indeed occur in the vascular compartment in the presence of salts, proteins, and enzymes. Micelle-based carriers may also collapse upon dilution in the blood stream [11]. Nanotheranostics below 10 nm are filtered out from the blood stream by rapid clearance through the glomerular capillaries of kidneys. Up to 500 nm and depending on the surface properties of the nanotheranostic system (charges, hydrophilicity, shape) opsonization may occur, followed by macrophage uptake and segregation in organs such as liver, spleen, and bone marrow. Different strategies were used to reduce the opsonization process including surface modification with polymers either natural, as polysaccharides (dextran, heparin, chitosan) [12,13] or synthetic, as polyethylene glycol (PEG) [14]. Extending the plasmatic half-life increases the probability for nanotheranostic systems to accumulate passively in the tumor by the Enhanced Permeation and Retention (EPR) Effect, which consists in the escape through leaky vasculature and the maximal retention due to defectuous lymphatic drainage. An interesting study about PEGylated liposomes (90 nm) labeled with gadolinium (Gd) chelates (^{1}H MRI probe) and loaded with siRNA demonstrated that the nanotheranostic accumulation in the tumor was sufficient after 24 h to reduce the growth of

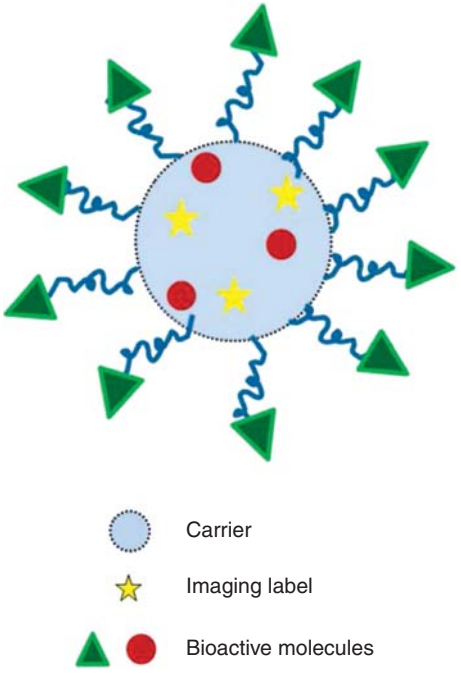

Figure 1. The three components of a typical nanotheranostic system: the carrier, the imaging label, and the bioactive molecule.

malignant cells [15]. Nanotheranostic systems consisting in hyperbranched-star amphiphilic fluoropolymers micelles were designed for ^{19}F MRI and doxorubicin (Dox) delivery [16,17]. Because of their smaller size, these micelles may extravasate more efficiently through fenestrated neovessels than larger particles. As shown by authors, they presented high loading capacities of Dox and good Signal-to-Noise Ratios (SNR) in MRI [16,17]. Unfortunately, the imaging acquisition was time-consuming, due to the limited ^{19}F concentration in the tumor and not transposable to clinics (several hours). The same strategy was further developed using PEG-grafted Poly(acrylic acid)-b-Poly(styrene)-co-Poly(2,3,4,5,6-pentafluorostyrene) [PAA-b-(PS-co-PPFS)], to increase the fluorine content on the polymer backbone, thus facilitate the imaging and to enhance the stealthiness of the micelle. However, this strategy revealed to be deceitful again, in terms of signal intensity with MRI [18].

Passive targeting encounters some limitations. In most cases, the proportion of nanotheranostics, which effectively reaches the tumor site, is rather low compared to the injected dose [19]. Moreover, hydrophilic PEGylated surfaces certainly protect the nanotheranostics from plasma proteins adsorption but also hamper internalization. Finally, the degree of tumor vascularization and porosity of vessels depend on the tumor type and the stage of development [5]. All the strategies to concentrate nanotheranostic systems in tumors cannot rely only on the EPR effect (**Figure 2**). Other strategies are needed to increase nanoparticle distribution within the tumor.

3. Nanotheranostics targeting the malignant cells

Active targeting overcomes the limitations mentioned above, by specifically attracting and/or binding nanotheranostics to malignant tissues, thus increasing their local concentration. Different physical, chemical, or biological approaches can be considered to, respectively, attract nanotheranostics by applying an external driving force (magnet); attach targeting ligands to the surface or to benefit of cells recruitment in the inflammatory tumor site.

The possibility to target a solid tumor with liposomes loaded with Superparamagnetic Iron Oxide (SPIO) nanoparticles by using an external gradient magnetic field was reported by several authors [20,21]. The magnet is typically positioned over the subcutaneously implanted tumor, leading to an accumulation of the nanotheranostics. In one case, particles' concentration was increased by 2.9 times [20]. In another case, the enhancement of the negative contrast was observed. The signal intensity decreased by 57 ± 12% instead of only 20 ± 5% without magnetic guidance [22]. This physical approach, added to the EPR effect, enhances nanotheranostic accumulation in the tumor. Nevertheless, this type of targeting is difficult to translate into clinics in situations where the magnet needs to be implanted because of the depth of the tumor site. This is the reason why the main approach consisting in targeting malignant tissue at the molecular scale, without the need of physical means, was importantly considered.

The most commonly developed chemical approach of active targeting is based on the ligand-receptor recognition that allows molecular imaging (**Figure 2**). The type of ligand used in nanotheranostic systems includes peptides [23,24], proteins [25], aptamers [26], or small molecules such as folic acid [27]. Advantages of active targeting are numerous. Nonspecific binding is avoided or at least minored compared to ligand-receptor interactions. An interesting ^{19}F MRI nanoprobe was developed by Takaoka *et al.* in which a head-ligand, such as biotin, coupled with CF_3 tail groups formed controlled aggregates in water. When specific recognition of the protein occurred, the aggregate disassembled, the CF_3 groups recovered mobility thus the ^{19}F MRI probe was turned on [28]. Another advantage resides in the possibility to distinguish bound from unbound nanosystem by properly setting the imaging parameters. The ^{19}F signal of vitronectin-modified Perfluoro Crown Ether (PFCE) emulsion circulating in the bloodstream was suppressed by a well-chosen diffusion-weighted MRI sequence, underlying the selective targeting of integrins $\alpha_v\beta_3$ *in vivo* [29]. The number of targeting ligands on one nanosystem can be optimized to benefit from cooperative effect as noticed by Anderson *et al.* with a highly echogenic decafluorobutane bubbles covalently coupled to a cRGD (cyclic Arg-Gly-Asp) peptide. They numbered ≈ 8.2×10^6 molecules of cRGD/bubble, which exhibited a five-fold higher adhesion to immobilized integrins, relative to nontargeted bubble or aspecific-targeted bubble [30]. Marsh

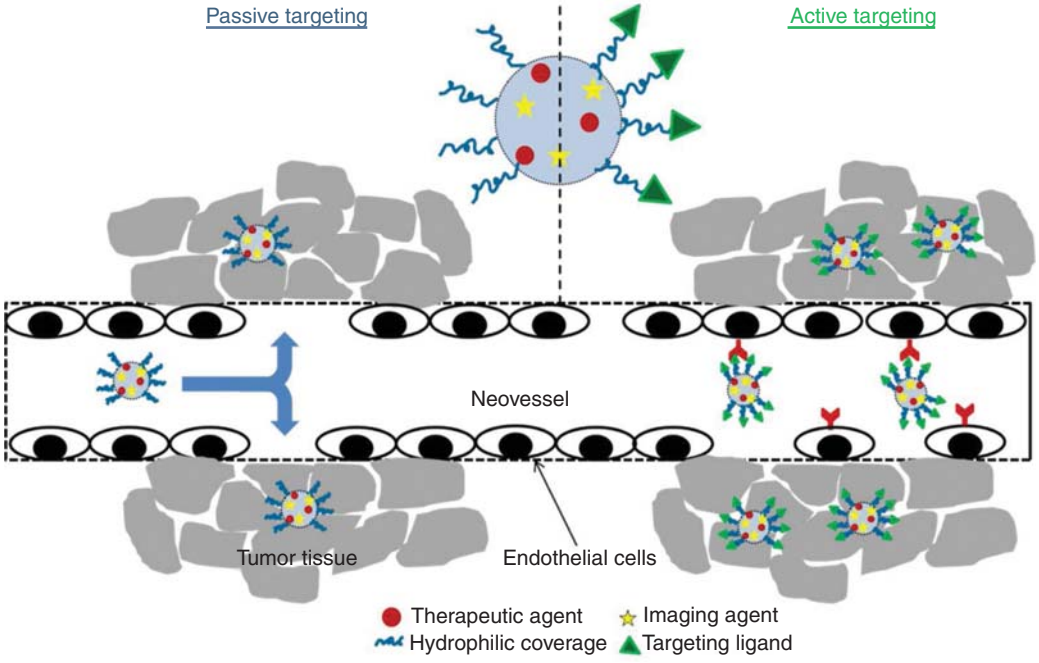

Figure 2. Passive and active targeting strategies for nanotheranostics to reach the tumor.

et al. characterized *in vitro* and *ex vivo* the interaction between biotinylated perfluorooctyl bromide (PFOB) nanoemulsion and avidin surfaces. They showed that multivalency increased the density of bound nanotheranostics to a surface, thus creating an extra reflective layer, which enhanced the imaging capabilities of the contrast agent for ultrasonography [31]. Finally, active targeting increases cellular uptake of nanotheranostics because it favors receptor-mediated endocytosis, as noticed by Kok *et al.* with a cRGD-nanoemulsion of PFCE. These authors studied the intracellular trafficking of their system by ^{1}H and ^{19}F MR imaging and spectroscopy. The targeted emulsion was internalized into vesicles in the perinuclear region whereas nontargeted emulsions were more evenly distributed within the cytoplasm [32]. The only downside aspect of active targeting is that it is often based on a probabilistic hypothesis. Biomarkers such as RGD peptides or folic acid are overexpressed by endothelial cells on neovessels or epithelial cells. Jokerst *et al.* considered that the differential of expression, between targeted and nontargeted tissues, of 2 to 10 was sufficient to ensure active targeting [33]. Nevertheless, healthy tissues may be affected. The expression level of the biomarkers also highly depends on the genetic pool of the patient and the disease development. Instead of overexpressed receptors, one should prefer, when it is possible, exclusive receptors for malignant cells, such as glypican (GPC), which is absent on normal adult tissue but highly expressed (80%) on hepatocellular carcinoma. Park *et al.* chose this strategy and evidenced the specific uptake by Hep G2 cancer cells using PEGylated SPIO nanoparticles coated with anti-GPC3 antibody [34].

Cell therapy was recently considered as a new approach to achieve active targeting. The first strategy exploits the tumor-homing properties of mesenchymal stem cells. As a wounded site, the tumor microenvironment consists of many signaling factors characteristic of an inflammatory site, such as vascular endothelial growth factor, fibroblast growth factor, interleukin-6, and cyclophilin-B [35]. Stem cells are then recruited to contribute to the healing process and promote tumorigenesis. They can be employed as nanoparticle carriers to actively deliver the therapeutic payload and the imaging agent to the tumor site. Indeed, stem cells were expanded and incubated *in vitro* with SPIO nanoparticles. These ^{1}H MRI contrast agents were internalized by endocytosis, entailing the cells themselves to serve as imaging agents. The labeling was almost 100% effective and had no effect on cell viability and proliferation [36]. Stem cells were also loaded either with PFCE or PFOB nanoemulsions. Once injected together, it was possible to differentiate and accurately quantify the two types of stem cells *in vivo*, because of the unequivocal and unique spectral signature of PFCE and PFOB through ^{19}F MR spectroscopy (**Figure 3**) [37,38].

Dendritic cells (DCs) are mainly used for cancer immunotherapy which can be loaded with relevant antigens as well as nanoparticles. After injection into patients, the DCs migrate to lymph nodes and stimulate T cells to activate an immune response. The functionality of DC strongly depends on their migratory ability. During one first clinical trial, the DCs were loaded with SPIO and administered to patients with melanoma. Despite a very elegant protocol,

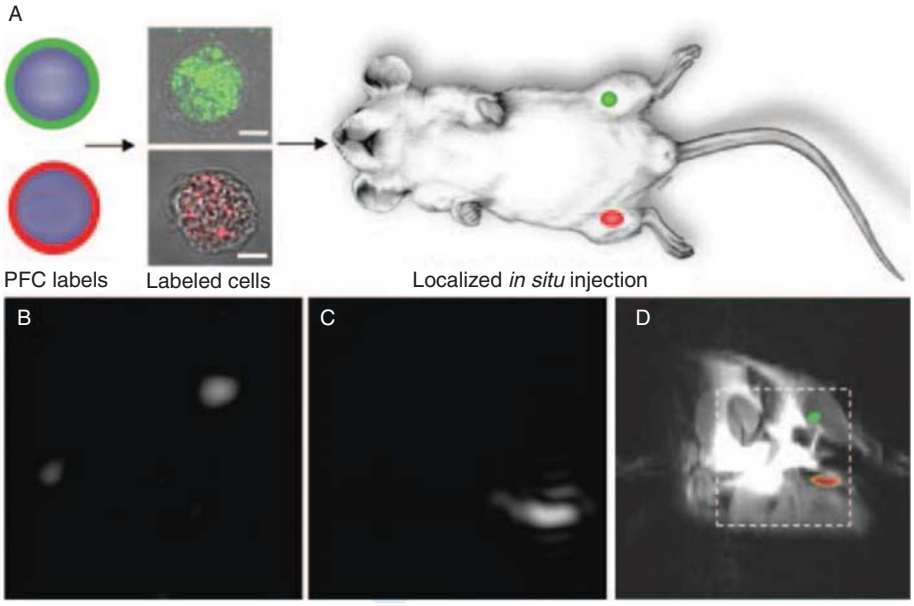

Figure 3. A) Stem cells were loaded either with PFOB or PFCE emulsions and injected into mouse thigh skeletal right or left muscle. B – C) ^{19}F MR imaging at 11.7 T (4 min scan time) by selecting the appropriate RF excitation frequencies for PFOB (B) and for PFCE (C). D) Overlay of B and C images onto a conventional ^{1}H anatomical image reveals PFOB and PFCE labeled cells localized to the left and right leg, respectively.

Reproduced from [37] with permission of The Journal of the Federation of American Societies for Experimental Biology.

the quantification of cells was hardly possible with MRI alone, thus requiring the additional use of scintigraphy [39]. ^{19}F MRI, which allows absolute quantification, was suggested to avoid the use of invasive imaging method. In this attempt, a commercially available perfluorocarbon (PFC) emulsion (CS 1000 Celsense, USA) was taken up by DCs, without cell toxicity and without the need of electroporation or transfer agents. The authors demonstrated the advantage of fluorinated contrast agent over typical ^{1}H MRI contrast agents, such as iron oxide or gadolinium, to suppress the background signal and improve the detection sensitivity of cells [40]. Macrophages or monocytes were also used for cell trafficking after *in vivo* injection. They were loaded with PFCE emulsion and shown to detect and monitor by ^{19}F MRI, graft rejection after solid organ transplantation [41], and with perfluorohexane (PFH) emulsion to image the cell capture by atherosclerotic plaque using ultrasonography [42].

4. Nanotheranostics for tumor reporting

Nanotheranostic systems targeted to neovessels should characterize the extent of angiogenesis and the delineation of the solid tumor [30,43]. Moreover, they should provide clear information about the specific tumor microenvironment (hypoxia, pH, enzymatic functions, and hypercalcemia). Indeed, poorly organized tumor vasculature and high oxygen demand of proliferative tumor cells are responsible for the common hypoxia of solid tumors. Hypoxic tumor cells are more resistant to radiotherapy and chemotherapy than their well-oxygenated counterparts [44]. Thus, mapping and understanding the degree of oxygenation in the targeted area is critical before considering the therapeutic aspects. As a matter of fact, PFCs combined with ^{19}F MRI were widely used for this purpose because of their high ability to dissolve oxygen. As oxygen possesses a paramagnetic effect [45], the partial pressure of dissolved O_2 (p_{O2}) in PFCs is linearly correlated with the ^{19}F longitudinal relaxivity (r1) of PFCs at a given temperature. Oxymetry studies were developed with hexafluorobenzene [46,47] directly injected into the tumor or with PFOB or perfluorodecalin encapsulated within nanoemulsions injected intravenously [48,49]. Thanks to the good spatial resolution of ^{19}F MRI, Diepart *et al.* evidenced heterogeneities in terms of oxygen consumption within the tumor and claimed they were able to anticipate the resistance to treatment of the poorly oxygen-supplied regions [47].

Other features of the tumor are its stimulated enzymatic activity [50] and acidic microenvironment. Indeed, protons are highly produced due to the intense metabolic activity of the tumor (glycolysis, glutaminolysis, ATP hydrolysis). Moreover, they are retained at high level, because of the poor lymphatic drainage, thus decreasing the local pH [51]. Numerous nano-^{19}F MRI probes were designed to respond accordingly to this pH variation. Oishi *et al.* developed a pH-sensitive PEGylated nanoparticle, containing a fluorinated gel core.

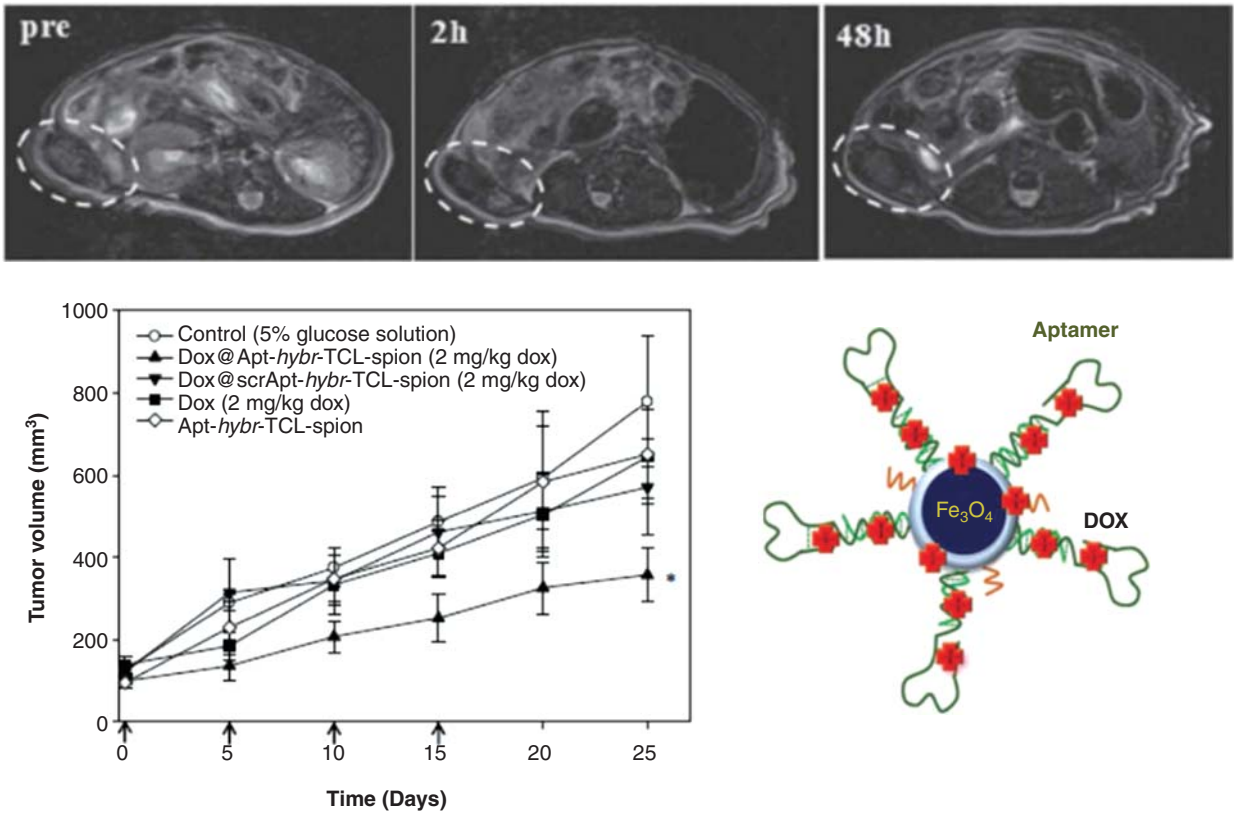

Figure 4. Top: T_2-weighted fast-spin echo images in the tumor (dashed circle) before injection and 2 and 48 h later. Bottom: Tumor growth for 25 days proving the antitumor activity of aptamer conjugated nanoparticles loaded with doxorubicin, which is represented on the right side.

Reproduced from [66] with permission of John Wiley & Sons, Inc.

At neutral pH, the probe was turned off because of the packed structure of the core, which hinders the motion of ^{19}F. At acidic pH, the fluorinated core recovered flexibility and the probe was turned on [52]. Mizukami *et al.* benefited of the strong metabolic activity of the tumor. They engineered ^{19}F MRI probe composed of a fluorine-containing group and a Gd-chelate, separated by a hydrolase cleavable linker, which was demonstrated to be sensitive to protease, caspase-3, and β-galactosidase. The interaction of the paramagnetic gadolinium with the ^{19}F moiety causes a shortening of the T2 by paramagnetic relaxation enhancement and, as a consequence, the ^{19}F MR signal is attenuated. After hydrolysis by enzymes and subsequent release of fluorine group, the ^{19}F signal increased [53]. Finally, calcium plays a significant role as a secondary messenger in cellular signaling pathways. Cell transition from normal to malignant state is a multistage process characterized by a major reorganization of active and passive Ca^{2+} cellular transport through pumps, exchangers, and canals [54]. Atanasijevic *et al.* developed a calcium-sensitive ^{1}H MRI contrast agent: nanoparticles loaded with calmodulin (calcium-binding protein) and SPIO. In the presence of calcium ions, nanoparticles aggregated and created transverse relaxivity changes (r2) on MR imaging [55].

5. Nanotheranostics for cancer therapy

Once targeted, imaged, and mapped, tumors should be treated and malignant cells eliminated. To achieve this goal, three different strategies may be considered: i) mechanical ablation (by surgery or physical external input), ii) chemotherapy, or iii) biological disruption using gene therapy for instance.

As for surgery, nanotheranostic systems, containing an imaging probe, diagnose the tumor type, location, and margins. As a matter of fact, the use of imaging methods can be considered as a stage of treatment, when it monitors and guides the tumor resection. Intraoperative imaging during surgery is particularly interesting because it assesses the extent of the tumor in real-time, improves the completeness of tumor removal, and reduces injury to the surrounding healthy tissues [43]. Unfortunately, some patients are unable to undergo surgical resection because of their poor physical condition or in case the tumor is not accessible. Thermal ablation might be an alternative solution to treat them. This method consists in applying a focused beam of thermal energy on tumor tissues, implying protein denaturation and coagulation necrosis. High Intensity Focused Ultrasounds (HIFU) can generate this energy. The technology has been used on thousands of patients

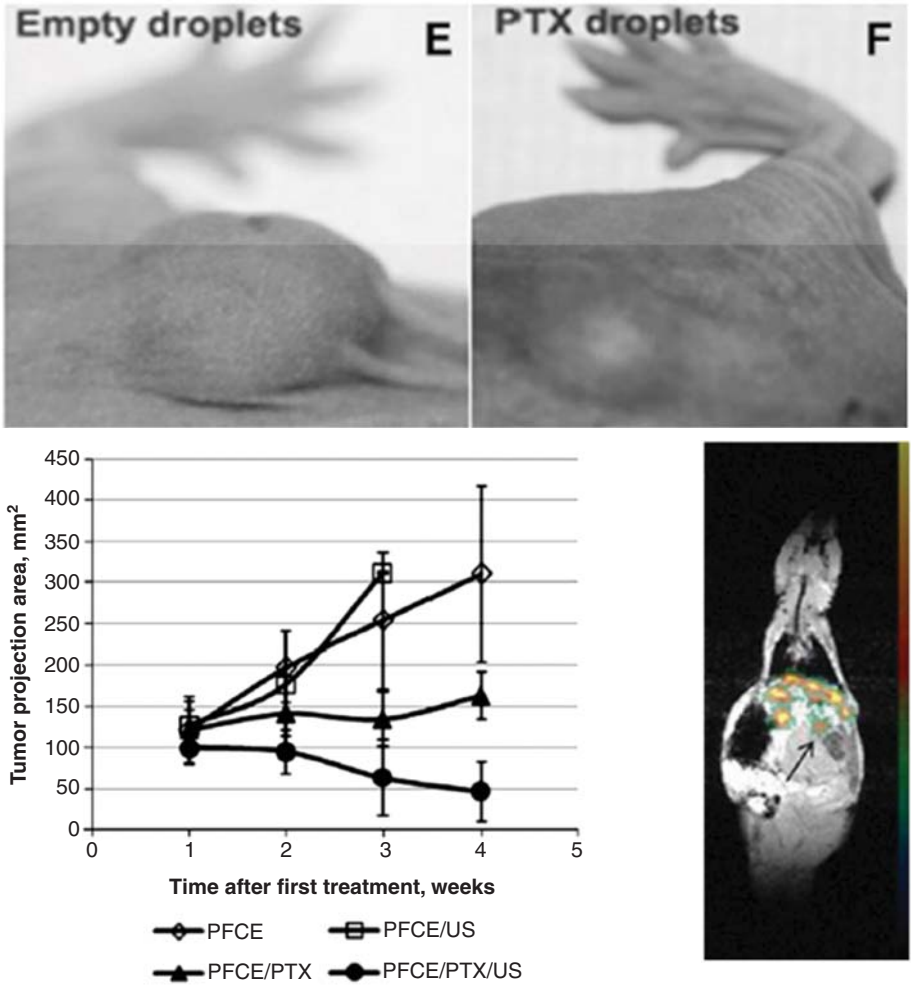

Figure 5. Top: Photographs of the subcutaneous tumor 12- days after treatment, which consisted in systemic administration of empty or paclitaxel-loaded droplets followed by focused ultrasound application. Bottom: Evolution of the tumor size for pancreatic cancer bearing mice treated with either empty (open symbols) or PTX-loaded PFCE nanodroplets (closed symbols). ^{19}F MR image superimposed with anatomical ^{1}H MR image of a coronal slice of the mouse after four systemical injections (every 2 h) of PFCE nanodroplets.

Reproduced from [67] with permission of Elsevier.

for the treatment of uterine fibroids, liver, breast, pancreatic, and other cancers [56]. It was moreover shown that the administration of US contrast microbubbles (Optison®) considerably lowered the energy threshold, by a factor of 12, for tissue damage with HIFU. Without contrast agents, an increase of 11.4°C was necessary to induce necrotic lesions, with 50% chance, whereas only a 5.9°C heating was required with Optison®. US contrast microbubbles enhanced the local energy absorption involving other mechanical mechanisms, like cavitation [57]. Furthermore, to accurately estimate the ablation margins by ultrasonography, during the ablation procedure, heat-sensitive decafluoropentane bubbles, which become hyperechogenic above 55°C, were engineered [58]. The thermal energy can also be produced by an alternative high-frequency magnetic field mediated by exothermic injected magnetic particles, so-called Magnetic Fluid Hyperthermia (MFH). Well-targeted to the tumor, the magnetic nanoparticles should precisely direct and control the heating at the cellular scale [59]. Several studies evidenced a significant reduction in tumor growth in mice [60,61]. MFH-based clinical trial was successfully conducted by Jordan *et al.* with patients affected by prostate carcinoma. After injection of SPIO nanoparticles, the radiofrequency treatment was monitored by ^{1}H MRI and Computed Tomography [62].

Traditionally, nanotheranostics are designed to carry chemotherapeutics such as doxorubicin, paclitaxel, and so forth. Drugs are incorporated by physical entrapment, in the aqueous or hydrophobic compartment of the carrier, or by chemical conjugation. These formulations led to a considerably increased local concentration of drug in the tumor, compared to free-drug injections [63,64]. Well-targeted, the nanotheranostic can release its payload in the tumor, by passive diffusion or

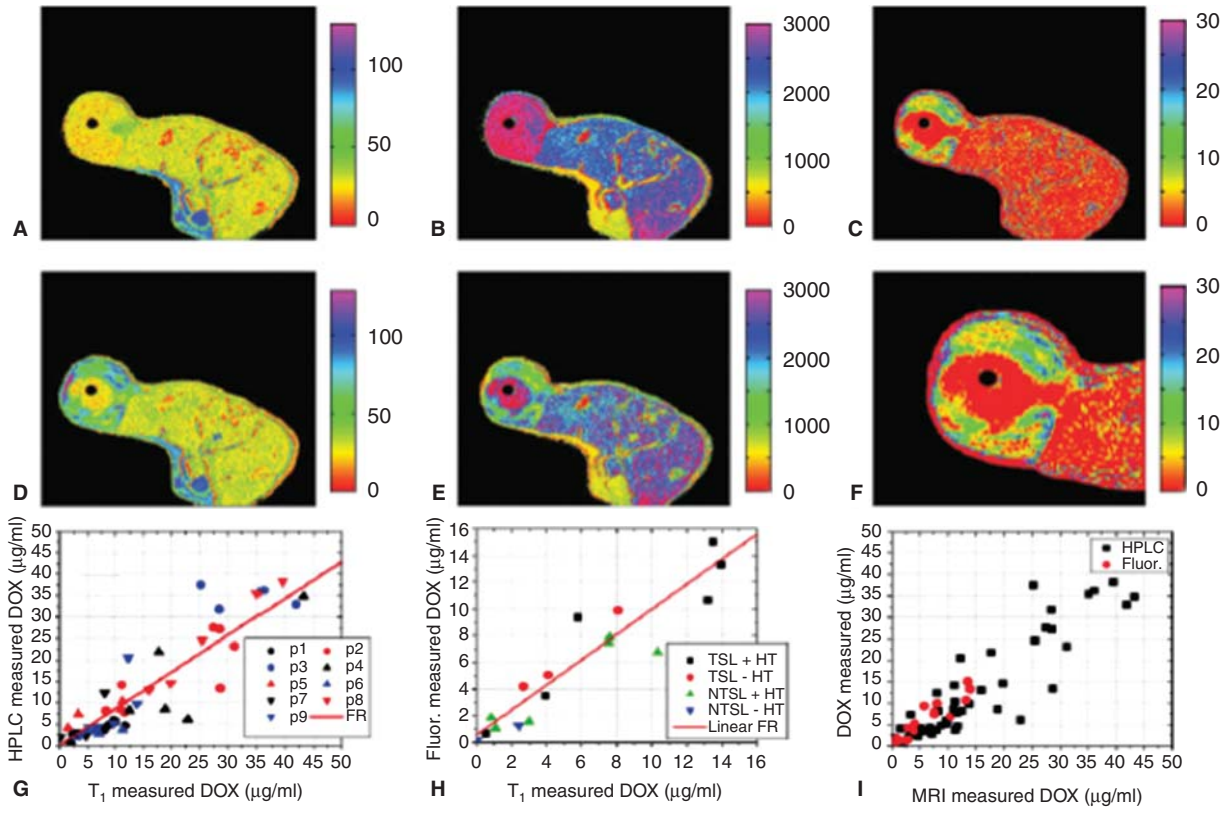

Figure 6. A) and **D)** Raw signal intensity maps show axial views of the rat bearing tumor with a central heating catheter at t = 0 min **(A)** and t = 45 min **(D)** after Dox-loaded liposomes injection. **B)** and **E)** T1 converted maps from **A)** and **D)**, respectively. **C)** Calculated Dox concentration from images **B** and **E**. **F)** Enlarged image of **C)** showing the heterogeneity in drug delivery within the tumor. **G)** and **H)** Linear correlation between HPLC and histological respectively with relaxivity measurements validated (Dox) measurements. **I)** Overlay of **G** and **H** showing the precision and accuracy of MRI for measuring Dox at low concentrations.

Reproduced from [74] with permission of John Wiley & Sons, Inc.

self-degradation (e.g., hydrolysis for PLGA nanoparticles). Several nanotheranostic systems already proved their efficacy *in vivo*, in terms of tumor growth reduction. Among them, the SPIO platforms are highly represented [65,66]. Yu *et al.* designed cross-linked SPIO nanoparticles functionalized with aptamers and loaded with doxorubicin. They evidenced a 53% relative signal enhancement in the tumor 2 h after injection, persisting even 48 h later, and a reduction of the tumor growth by a factor 2 (**Figure 4**). Rapoport *et al.* used PFCE nanoemulsions loaded with paclitaxel to image, by ^{19}F MRI, and to treat orthotopically inoculated pancreatic tumor. They underlined their difficulties to attribute the ^{19}F MR signal to the tumor, liver tissues, or liver metastases. A better specific targeting approach would solve this problem. Nevertheless they demonstrated the high therapeutic potential of their system by a substantial tumor regression and metastases suppression using ultrasound-mediated chemotherapy (**Figure 5**) [67]. Instead of the usual drugs, Soman *et al.* reported the delivery of a cytolytic peptide: melittin, by a PFOB lipid nanoparticle, imaged by ^{19}F MR molecular imaging [68]. Moreover, the system allowed accumulation of melittin in murine tumors *in vivo* and a dramatic reduction in tumor growth without any apparent signs of toxicity [69]. Imaging the drug release is of utmost importance to achieve effective treatment. This is easily done *in vitro* or *ex vivo* [70-72] but the examples are scarcer *in vivo*. Onuky *et al.* visualized by ^{1}H MRI in xenograft mice, the release of 5-fluorouracil from PLGA nanoparticles, carrying additional two imaging probes: Gd-DTPA and SPIO [73]. Viglianti *et al.* performed a particularly relevant and meticulous analysis of the release of doxorubicin from liposomes, coencapsulated with manganese as the MRI contrast agent. They linearly correlated the increase of longitudinal relaxivity (r1) by MR spectroscopy to the doxorubicin local concentrations in the tumor, by confronting the HPLC and histological measurements (**Figure 6**). This method is a promising approach for imaging drug efficacy and real-time evaluation of chemotherapeutic protocols [74].

Beside passive approaches, active control of release is possible through several means. It is possible at first to exploit the high enzymatic activity and acidic conditions of the tumor

microenvironment. This effect was exploited by Castelletto *et al.* by covalently binding a drug to a micellar carrier. The drug was released by hydrolytic cleavage due to chymotrypsin [75]. pH-sensitive nanoparticles of fluorinated dendrimers, imaged by ^{19}F MRI, were disassembled at pH 6, enabling controlled release of physically entrapped payload [76]. Acidic pH can affect the drug molecule itself. For example, protonation of doxorubicin (Dox) increased its water solubility, thus weakened interactions with hydrophobic targeted SPIO nanoparticle and speeded up the release [77].

Some authors also demonstrated the huge benefit of ultrasounds on the release of Dox from polymeric nanobubbles of perfluoropentane (PFP), thus increasing tumor inhibition *in vivo* [78]. Several other groups used ultrasounds as an external force to actively trigger drug release [30,79]. Two different effects should be considered apart: the assimilated sonoporation and the direct cavitation. In the first case, the drug was loaded within a liquid/solid nanoparticle. The application of oscillating Low Frequencies US, created air bubbles nuclei within the particle (in membrane or aqueous core of liposome for example). These small air bubbles cavitated, thus opening transient pores through the drug carrier, allowing small therapeutic molecules to diffuse in more efficiently [80,81]. In the second case, the drug was initially encapsulated in a nanoparticle containing a gaseous core. The nanotheranostic system underwent oscillations followed by a cavitation process, exploded, and released its therapeutic payload [70].

Finally, the external input of energy may induce a phase transition in the nanotheranostic. Many PFC liquid core nanoparticles were designed to become gaseous when insonified, because of the combined effects of local increased acoustic pressure and temperature. This phenomenon is called the Acoustic Droplet Vaporization (ADV). Several groups evidenced the droplet to bubble conversion, followed by cavitation, inducing the release of camptothecin or thrombin, for example [82,83]. Usually PFP or PFH are used for ADV because of their low boiling points: T = 29°C and T = 59°C, respectively. Nevertheless, Rapoport and Mohan reported ADV with their PFCE-core nanoparticles, while the boiling point of PFCE is 146°C. In another way, phase transition can concern the carrier instead of the imaging agent. This concept was applied to liposomes, which undergo a gel-to-liquid phase transition at a critical temperature. Above this temperature, the mobility of lipids is increased within the membrane and small molecules can diffuse throughout. The heating stimulus can be provided either by pulsed-HIFU [84,85] or by hyperthermia with an oscillating magnetic field [86]. Langereis and Grüll monitored, by MR-HIFU, the controlled release of drug from a temperature-sensitive liposome with commutative imaging capabilities. Chemical Exchange Saturation Transfer (CEST) signal is replaced by ^{19}F MRI signal upon reaching the melting temperature of the lipid membrane, after sonication [87,88].

Gene delivery is seriously considered for cancer therapy because more than just regulating its propagation, it tackles the disease from the causes and origins. DNA delivery, mediated by a plasmid, aims to replace a damaged gene with a functional counterpart, to restore normal cell function or to induce a new function. On the contrary, SiRNA delivery aims to knockdown the expression of proteins such as oncogenes. Many nanotheranostics were designed to deliver plasmid DNA or siRNA [89-91]. Magnetic nanoparticles targeted to breast adenocarcinomas using the EPPT (Glu-Pro-Pro-Ther) peptide were loaded with siRNA to induce apoptosis of malignant cells and thus reduced significantly the tumor growth [24]. 3D-cultured breast cancer cells, which well-mimic the *in vivo* conditions and provide reproducible and controlled experimental conditions, were imaged by ^{19}F MRI. This study allowed Bartusik *et al.* to distinguish the more efficient therapeutic formulation of Herceptin-targeted emulsions containing a core of PFC and lipoplex, complexing the plasmid [92,93]. Lee *et al.* used manganese-doped iron oxide nanoparticles for SiRNA delivery. They underlined the problem to monitor the intracellular transfection by ^{1}H MRI. This requires indeed probing the deep inside of the cell structure, and MRI spatial resolution is not low enough: innate limit is 100 µm. Fluorescent imaging was needed for subcellular trafficking [94].

6. Conclusion

Nanotheranostic systems provide a unique opportunity to hinder devastating effects of cancer, which affects millions of people yearly. They can be designed to specifically interact with malignant cells, image them, trigger a therapeutic response, and monitor it in real-time. The treatment protocol (dosing, type, and time) can be adjusted based on tumor and off-target tissue accumulation. The nanotheranostics will be upgraded from preclinical research to clinical application if the toxicity issues are better predicted and the scale-up and engineering of these complex structures are profitable. Microfluidic platforms were already mentioned to synthesize, in reproducible manner, a substantial batch of nanoparticles and screen their biophysicochemical features [95].

7. Expert opinion

In the last 20 years, progress in formulation science and physicochemistry has allowed the controlled and reproducible production of nanoparticles. Additional knowledge in organic and biomolecular chemistry has rendered possible surface modification (i.e., decoration) of nanoparticles, reducing their clearance by the immune system and making them more compatible with *in vivo* uses. By this multidisciplinary approach, multifunctional nanocarriers were designed and imaging probes, as well as therapeutic agents, were custom-built incorporated. Cancer is a worldwide public health concern and significant health care resources are spent on diagnosis. Sooner the detection of the tumor better is the chance of remission without relapse. In this context, nanotheranostics

offer a panel of solutions for the development of personalized cancer therapy. MRI and ultrasonography are used to detect a broad range of cancers (breast, colon, brain, etc.). Nevertheless the use of these techniques in combination with nanotheranostics agents is challenging, mostly because the local concentration reached in the tumor is often below the sensitivity detection range. Indeed, echogenicity suffer from the downscaling to nanometer range of contrast agents. That is the reason why commercialized ultrasound contrast agents still consist in microbubbles. Concerning MRI, an interesting move was made toward the fluorine imaging. In this case, there is no endogenous background signal and the signature of exogenous fluorinated contrast agent is unique and specific, lowering the detection sensitivity to 1 mM. But MRI still lack of spatial resolution. Computed tomography-based fluorine may be a solution but many researchers prefer to focus on fluorescence imaging. The therapeutic efficacy of nanotheranostics was successfully demonstrated, mostly in an indirect way, considering for instance the tumor regression. Nevertheless, direct imaging of drug release at the targeted site still remains difficult. The choice of the targeted strategy should be seriously considered. However, to achieve this goal, the specificity of biomarkers should be improved and ligands that do not induce immunogenic response should be designed. Finally, to provide personalized medicine, the patient condition should be considered. The intravenous administration requires hospitalization, which generates important costs and is less flexible than ambulatory care. Thus, it would be interesting to develop needleless approaches of nanotheranostic administration. The pulmonary route is attractive because it is noninvasive and allows both local treatment for lung cancer and systemic drug absorption through lung capillaries. Additional to personalized medicine, ensuring convenience and improving the quality of life would be optimistic promises to numerous patients.

Declaration of interest

The authors state no conflict of interest and have received no payment in preparation of this manuscript.

Bibliography

1. Ponce AM, Viglianti BL, Yu D, et al. Magnetic resonance imaging of temperature-sensitive liposome release: drug dose painting and antitumor effects. J Natl Cancer Inst 2007;99(1):53-63
2. de Smet M, Heijman E, Langereis S, et al. Magnetic resonance imaging of high intensity focused ultrasound mediated drug delivery from temperature-sensitive liposomes: an in vivo proof-of-concept study. J Control Release 2011;150(1):102-10
3. Bates S. Progress towards personalized medicine. Drug Discov Today 2010;15(3-4):115-20
4. Barreto JA, O'Malley W, Kubeil M, et al. Nanomaterials: applications in cancer imaging and therapy. Adv Mater 2011;23(12):H18-40
5. Bae KH, Chung HJ, Park TG. Nanomaterials for cancer therapy and imaging. Mol Cells 2011;31(4):295-302
6. Kateb B, Chiu K, Black KL, et al. Nanoplatforms for constructing new approaches to cancer treatment, imaging, and drug delivery: what should be the policy? Neuroimage 2011;54(Suppl 1):S106-24
7. Keupp J, Rahmer J, Grasslin I, et al. Simultaneous dual-nuclei imaging for motion corrected detection and quantification of 19F imaging agents. Magn Reson Med 2011;66(4):1116-22
8. Hu L, Hockett FD, Chen J, et al. A generalized strategy for designing (19) F/(1)H dual-frequency MRI coil for small animal imaging at 4.7 Tesla. J Magn Reson Imaging 2011;34(1):245-52
9. Neubauer AM, Myerson J, Caruthers SD, et al. Gadolinium-modulated 19F signals from perfluorocarbon nanoparticles as a new strategy for molecular imaging. Magn Reson Med 2008;60(5):1066-72
10. Fang C, Bhattarai N, Sun C, et al. Functionalized nanoparticles with long-term stability in biological media. Small 2009;5(14):1637-41
11. Bhadra D, Bhadra S, Jain NK. Pegylated lysine based copolymeric dendritic micelles for solubilization and delivery of artemether. J Pharm Pharm Sci 2005;8(3):467-82
12. Alhareth K, Vauthier C, Bourasset F, et al. Conformation of surface-decorating dextran chains affects the pharmacokinetics and biodistribution of doxorubicin-loaded nanoparticles. Eur J Pharm Biopharm 2012;81(2):453-7
13. Amoozgar Z, Park J, Lin Q, et al. Low molecular-weight chitosan as a pH-sensitive stealth coating for tumor-specific drug delivery. Mol Pharm 2012;9(5):1262-70
14. Jokerst JV, Lobovkina T, Zare RN, et al. Nanoparticle PEGylation for imaging and therapy. Nanomedicine (Lond) 2011;6(4):715-28
15. Kenny GD, Kamaly N, Kalber TL, et al. Novel multifunctional nanoparticle mediates siRNA tumour delivery, visualisation and therapeutic tumour reduction in vivo. J Control Release 2011;149(2):111-16
16. Du W, Nystrom AM, Zhang L, et al. Amphiphilic hyperbranched fluoropolymers as nanoscopic 19F magnetic resonance imaging agent assemblies. Biomacromolecules 2008;9(10):2826-33
17. Du W, Xu Z, Nystrom AM, et al. 19F- and fluorescently labeled micelles as nanoscopic assemblies for chemotherapeutic delivery. Bioconjug Chem 2008;19(12):2492-8
18. Nystrom AM, Bartels JW, Du W, et al. Perfluorocarbon-loaded shell crosslinked knedel-like nanoparticles: lessons regarding polymer mobility and self assembly. J Polym Sci A Polym Chem 2009;47(4):1023-37
19. Diou O, Tsapis N, Giraudeau C, et al. Long-circulating perfluorooctyl bromide nanocapsules for tumor imaging by 19FMRI. Biomaterials 2012;33(22):5593-602

20. Kuznetsov AA, Filippov VI, Alyautdin RN, et al. Application of magnetic liposomes for magnetically guided transport of muscle relaxants and anti-cancer photodynamic drugs. J Magn Magn Mater 2001;225(1-2):95-100

21. Fortin-Ripoche JP, Martina MS, Gazeau F, et al. Magnetic targeting of magnetoliposomes to solid tumors with MR imaging monitoring in mice: feasibility. Radiology 2006;239(2):415-24

22. Gultepe E, Reynoso FJ, Jhaveri A, et al. Monitoring of magnetic targeting to tumor vasculature through MRI and biodistribution. Nanomedicine (Lond) 2010;5(8):1173-82

23. Medarova Z, Rashkovetsky L, Pantazopoulos P, et al. Multiparametric monitoring of tumor response to chemotherapy by noninvasive imaging. Cancer Res 2009;69(3):1182-9

24. Kumar M, Yigit M, Dai G, et al. Image-guided breast tumor therapy using a small interfering RNA nanodrug. Cancer Res 2010;70(19):7553-61

25. Bartlett DW, Su H, Hildebrandt IJ, et al. Impact of tumor-specific targeting on the biodistribution and efficacy of siRNA nanoparticles measured by multimodality in vivo imaging. Proc Natl Acad Sci USA 2007;104(39):15549-54

26. Wang AZ, Bagalkot V, Vasilliou CC, et al. Superparamagnetic iron oxide nanoparticle-aptamer bioconjugates for combined prostate cancer imaging and therapy. ChemMedChem 2008;3(9):1311-15

27. Yang X, Grailer JJ, Rowland IJ, et al. Multifunctional SPIO/DOX-loaded wormlike polymer vesicles for cancer therapy and MR imaging. Biomaterials 2010;31(34):9065-73

28. Takaoka Y, Kiminami K, Mizusawa K, et al. Systematic study of protein detection mechanism of self-assembling 19F NMR/MRI nanoprobes toward rational design and improved sensitivity. J Am Chem Soc 2011;133(30):11725-31

29. Waters EA, Chen J, Yang X, et al. Detection of targeted perfluorocarbon nanoparticle binding using 19F diffusion weighted MR spectroscopy. Magn Reson Med 2008;60(5):1232-6

30. Anderson CR, Hu X, Zhang H, et al. Ultrasound molecular imaging of tumor angiogenesis with an integrin targeted microbubble contrast agent. Invest Radiol 2011;46(4):215-24

31. Marsh JN, Partlow KC, Abendschein DR, et al. Molecular imaging with targeted perfluorocarbon nanoparticles: quantification of the concentration dependence of contrast enhancement for binding to sparse cellular epitopes. Ultrasound Med Biol 2007;33(6):950-8

32. Kok MB, de Vries A, Abdurrachim D, et al. Quantitative (1)H MRI, (19)F MRI, and (19)F MRS of cell-internalized perfluorocarbon paramagnetic nanoparticles. Contrast Media Mol Imaging 2011;6(1):19-27

33. Jokerst JV, Gambhir SS. Molecular imaging with theranostic nanoparticles. Acc Chem Res 2011;44(10):1050-60

34. Park JO, Stephen Z, Sun C, et al. Glypican-3 targeting of liver cancer cells using multifunctional nanoparticles. Mol Imaging 2011;10(1):69-77

35. El-Haibi CP, Karnoub AE. Mesenchymal stem cells in the pathogenesis and therapy of breast cancer. J Mammary Gland Biol Neoplasia 2010;15(4):399-409

36. Chen R, Yu H, Jia ZY, et al. Efficient nano iron particle-labeling and noninvasive MR imaging of mouse bone marrow-derived endothelial progenitor cells. Int J Nanomedicine 2011;6:511-19

37. Partlow KC, Chen J, Brant JA, et al. 19F magnetic resonance imaging for stem/progenitor cell tracking with multiple unique perfluorocarbon nanobeacons. FASEB J 2007;21(8):1647-54

38. Ruiz-Cabello J, Walczak P, Kedziorek DA, et al. In vivo "hot spot" MR imaging of neural stem cells using fluorinated nanoparticles. Magn Reson Med 2008;60(6):1506-11

39. de Vries IJM, Lesterhuis WJ, Barentsz JO, et al. Magnetic resonance tracking of dendritic cells in melanoma patients for monitoring of cellular therapy. Nat Biotechnol 2005;23(11):1407-13

40. Bonetto F, Srinivas M, Heerschap A, et al. A novel (19)F agent for detection and quantification of human dendritic cells using magnetic resonance imaging. Int J Cancer 2011;129(2):365-73

41. Hitchens TK, Ye Q, Eytan DF, et al. 19F MRI detection of acute allograft rejection with in vivo perfluorocarbon labeling of immune cells. Magn Reson Med 2011;65(4):1144-53

42. Kornmann LM, Curfs DM, Hermeling E, et al. Perfluorohexane-loaded macrophages as a novel ultrasound contrast agent: a feasibility study. Mol Imaging Biol 2008;10(5):264-70

43. Kircher MF, Mahmood U, King RS, et al. A multimodal nanoparticle for preoperative magnetic resonance imaging and intraoperative optical brain tumor delineation. Cancer Res 2003;63(23):8122-5

44. Davda S, Bezabeh T. Advances in methods for assessing tumor hypoxia in vivo: implications for treatment planning. Cancer Metastasis Rev 2006;25(3):469-80

45. Parhami P, Fung BM. F-19 Relaxation study of perfluoro chemicals as oxygen carriers. J Phys Chem Us 1983;87(11):1928-31

46. Liu S, Shah SJ, Wilmes LJ, et al. Quantitative tissue oxygen measurement in multiple organs using 19F MRI in a rat model. Magn Reson Med 2011;66(6):1722-30

47. Diepart C, Magat J, Jordan BF, et al. In vivo mapping of tumor oxygen consumption using (19)F MRI relaxometry. NMR Biomed 2011;24(5):458-63

48. Giraudeau C, Djemai B, Ghaly MA, et al. High sensitivity 19F MRI of a perfluorooctyl bromide emulsion: application to a dynamic biodistribution study and oxygen tension mapping in the mouse liver and spleen. NMR Biomed 2012;25(4):654-60

49. Mason RP, Antich PP. Tumor oxygen tension: measurement using oxygent as a 19F NMR probe at 4.7 T. Artif Cells Blood Substit Immobil Biotechnol 1994;22(4):1361-7

50. Aguilera TA, Olson ES, Timmers MM, et al. Systemic in vivo distribution of activatable cell penetrating peptides is superior to that of cell penetrating peptides. Integr Biol (Camb) 2009;1(5-6):371-81

51. Vaupel P, Kallinowski F, Okunieff P. Blood flow, oxygen and nutrient supply, and metabolic microenvironment of human tumors: a review. Cancer Res 1989;49(23):6449-65

52. Oishi M, Sumitani S, Nagasaki Y. On-off regulation of 19F magnetic resonance signals based on pH-sensitive PEGylated nanogels for potential tumor-specific smart 19F MRI probes. Bioconjug Chem 2007;18(5):1379-82

53. Mizukami S, Takikawa R, Sugihara F, et al. Paramagnetic relaxation-based 19f MRI probe to detect protease activity. J Am Chem Soc 2008;130(3):794-5

54. Berridge MJ, Bootman MD, Roderick HL. Calcium signalling: dynamics, homeostasis and remodelling. Nat Rev Mol Cell Biol 2003;4(7):517-29

55. Atanasijevic T, Shusteff M, Fam P, et al. Calcium-sensitive MRI contrast agents based on superparamagnetic iron oxide nanoparticles and calmodulin. Proc Natl Acad Sci USA 2006;103(40):14707-12

56. Orsi F, Arnone P, Chen W, et al. High intensity focused ultrasound ablation: a new therapeutic option for solid tumors. J Cancer Res Ther 2010;6(4):414-20

57. McDannold NJ, Vykhodtseva NI, Hynynen K. Microbubble contrast agent with focused ultrasound to create brain lesions at low power levels: MR imaging and histologic study in rabbits. Radiology 2006;241(1):95-106

58. Huang J, Xu JS, Xu RX. Heat-sensitive microbubbles for intraoperative assessment of cancer ablation margins. Biomaterials 2010;31(6):1278-86

59. Lartigue L, Innocenti C, Kalaivani T, et al. Water-dispersible sugar-coated iron oxide nanoparticles. An evaluation of their relaxometric and magnetic hyperthermia properties. J Am Chem Soc 2011;133(27):10459-72

60. Rachakatla RS, Balivada S, Seo GM, et al. Attenuation of mouse melanoma by A/C magnetic field after delivery of bi-magnetic nanoparticles by neural progenitor cells. ACS Nano 2010;4(12):7093-104

61. Hilger I, Hiergeist R, Hergt R, et al. Thermal ablation of tumors using magnetic nanoparticles: an in vivo feasibility study. Invest Radiol 2002;37(10):580-6

62. Gneveckow U, Jordan A, Scholz R, et al. Description and characterization of the novel hyperthermia- and thermoablation-system MFH 300F for clinical magnetic fluid hyperthermia. Med Phys 2004;31(6):1444-51

63. Waite CL, Roth CM. Nanoscale drug delivery systems for enhanced drug penetration into solid tumors: current progress and opportunities. Crit Rev Biomed Eng 2012;40(1):21-41

64. Blanco E, Hsiao A, Ruiz-Esparza GU, et al. Molecular-targeted nanotherapies in cancer: enabling treatment specificity. Mol Oncol 2011;5(6):492-503

65. Yang J, Lee CH, Ko HJ, et al. Multifunctional magneto-polymeric nanohybrids for targeted detection and synergistic therapeutic effects on breast cancer. Angew Chem Int Ed Engl 2007;46(46):8836-9

66. Yu MK, Kim D, Lee IH, et al. Image-guided prostate cancer therapy using aptamer-functionalized thermally cross-linked superparamagnetic iron oxide nanoparticles. Small 2011;7(15):2241-9

67. Rapoport N, Nam KH, Gupta R, et al. Ultrasound-mediated tumor imaging and nanotherapy using drug loaded, block copolymer stabilized perfluorocarbon nanoemulsions. J Control Release 2011;153(1):4-15

68. Soman NR, Lanza GM, Heuser JM, et al. Synthesis and characterization of stable fluorocarbon nanostructures as drug delivery vehicles for cytolytic peptides. Nano Lett 2008;8(4):1131-6

69. Soman NR, Baldwin SL, Hu G, et al. Molecularly targeted nanocarriers deliver the cytolytic peptide melittin specifically to tumor cells in mice, reducing tumor growth. J Clin Invest 2009;119(9):2830-42

70. Eisenbrey JR, Huang P, Hsu J, et al. Ultrasound triggered cell death in vitro with doxorubicin loaded poly lactic-acid contrast agents. Ultrasonics 2009;49(8):628-33

71. Gautier J, Munnier E, Paillard A, et al. A pharmaceutical study of doxorubicin-loaded PEGylated nanoparticles for magnetic drug targeting. Int J Pharm 2012;423(1):16-25

72. Kamm YJ, Heerschap A, Rosenbusch G, et al. 5-Fluorouracil metabolite patterns in viable and necrotic tumor areas of murine colon carcinoma determined by 19F NMR spectroscopy. Magn Reson Med 1996;36(3):445-50

73. Onuki Y, Jacobs I, Artemov D, et al. Noninvasive visualization of in vivo release and intratumoral distribution of surrogate MR contrast agent using the dual MR contrast technique. Biomaterials 2010;31(27):7132-8

74. Viglianti BL, Ponce AM, Michelich CR, et al. Chemodosimetry of in vivo tumor liposomal drug concentration using MRI. Magn Reson Med 2006;56(5):1011-18

75. Castelletto V, McKendrick JE, Hamley IW, et al. PEGylated amyloid peptide nanocontainer delivery and release system. Langmuir 2010;26(14):11624-7

76. Criscione JM, Le BL, Stern E, et al. Self-assembly of pH-responsive fluorinated dendrimer-based particulates for drug delivery and noninvasive imaging. Biomaterials 2009;30(23-24):3946-55

77. Zou P, Yu Y, Wang YA, et al. Superparamagnetic iron oxide nanotheranostics for targeted cancer cell imaging and pH-dependent intracellular drug release. Mol Pharm 2010;7(6):1974-84

78. Du L, Jin Y, Zhou W, et al. Ultrasound-triggered drug release and enhanced anticancer effect of doxorubicin-loaded poly(D,L-lactide-co-glycolide)-methoxy-poly(ethylene glycol) nanodroplets. Ultrasound Med Biol 2011;37(8):1252-8

79. Chappell JC, Song J, Burke CW, et al. Targeted delivery of nanoparticles bearing fibroblast growth factor-2 by ultrasonic microbubble destruction for therapeutic arteriogenesis. Small 2008;4(10):1769-77

80. Klibanov AL, Shevchenko TI, Raju BI, et al. Ultrasound-triggered release of materials entrapped in microbubble-liposome constructs: a tool for targeted drug delivery. J Control Release 2010;148(1):13-17

81. Schroeder A, Kost J, Barenholz Y. Ultrasound, liposomes, and drug delivery: principles for using ultrasound to control the release of drugs from liposomes. Chem Phys Lipids 2009;162(1-2):1-16

82. Fabiilli ML, Lee JA, Kripfgans OD, et al. Delivery of water-soluble drugs using acoustically triggered perfluorocarbon double emulsions. Pharm Res 2010;27(12):2753-65

83. Fang JY, Hung CF, Hua SC, et al. Acoustically active perfluorocarbon nanoemulsions as drug delivery carriers for camptothecin: drug release and cytotoxicity against cancer cells. Ultrasonics 2009;49(1):39-46

84. Dromi S, Frenkel V, Luk A, et al. Pulsed-high intensity focused ultrasound and low temperature-sensitive liposomes for enhanced targeted drug delivery and antitumor effect. Clin Cancer Res 2007;13(9):2722-7

85. Negussie AH, Yarmolenko PS, Partanen A, et al. Formulation and characterisation of magnetic resonance imageable thermally sensitive liposomes for use with magnetic resonance-guided high intensity focused ultrasound. Int J Hyperther 2011;27(2):140-55

86. Babincova M, Cicmanec P, Altanerova V, et al. AC-magnetic field controlled drug release from magnetoliposomes: design of a method for site-specific chemotherapy. Bioelectrochemistry 2002;55(1-2):17-19

87. Langereis S, Keupp J, van Velthoven JL, et al. A temperature-sensitive liposomal 1H CEST and 19F contrast agent for MR image-guided drug delivery. J Am Chem Soc 2009;131(4):1380-1

88. Grull H, Langereis S. Hyperthermia-triggered drug delivery from temperature-sensitive liposomes using MRI-guided high intensity focused ultrasound. J Control Release 2012;161(2):317-27

89. Kievit FM, Zhang M. Cancer nanotheranostics: improving imaging and therapy by targeted delivery across biological barriers. Adv Mater 2011;23(36):H217-47

90. Veiseh O, Kievit FM, Fang C, et al. Chlorotoxin bound magnetic nanovector tailored for cancer cell targeting, imaging, and siRNA delivery. Biomaterials 2010;31(31):8032-42

91. Liu G, Swierczewska M, Lee S, et al. Functional nanoparticles for molecular imaging guided gene delivery. Nano Today 2010;5(6):524-39

92. Bartusik D, Tomanek B. Application of 19F magnetic resonance to study the efficacy of fluorine labeled drugs in the three-dimensional cultured breast cancer cells. Arch Biochem Biophys 2010;493(2):234-41

93. Bartusik D, Tomanek B. Detection of fluorine labeled herceptin using cellular (19)F MRI ex vivo. J Pharm Biomed Anal 2010;51(4):894-900

94. Lee JH, Lee K, Moon SH, et al. All-in-one target-cell-specific magnetic nanoparticles for simultaneous molecular imaging and siRNA delivery. Angew Chem Int Ed Engl 2009;48(23):4174-9

95. Valencia PM, Basto PA, Zhang L, et al. Single-step assembly of homogenous lipid-polymeric and lipid-quantum dot nanoparticles enabled by microfluidic rapid mixing. ACS Nano 2010;4(3):1671

Affiliation

Odile Diou[1,2], Nicolas Tsapis[1,2] & Elias Fattal[†1,2]
[†]Author for correspondence
[1]University Paris-Sud,
LabEx LERMIT,
Faculté de Pharmacie,
5 rue J.B. Clément,
92296 Châtenay-Malabry Cedex,
France
Tel: +33146835568;
E-mail: elias.fattal@u-psud.fr
[2]CNRS UMR 8612,
Institut Galien Paris-Sud,
LabEx LERMIT,
5 rue J.B. Clément,
92296 Châtenay-Malabry Cedex,
France